knowledge that a large aspect ratio for the finite element quadrilaterals should be avoided. The extreme case presented, $\eta/t = 0.02$, $l/t = 20$, has an aspect ratio of 100:1. A check was made by recomputing the stresses using an aspect ratio of 40:1, with essentially no difference in the shearing stress distribution and hence no difference in the shearing stress concentration factor. The tearing stress distributions computed in the two cases differed only in the region near the reentrant corner where high stress gradients exist. Extrapolating the centroidal values of the stress to the surface requires considerable judgement. In both cases the curves are nearly vertical, but the smaller aspect ratio unquestionably yields larger tearing stress concentration factors. The authors hope that the curves presented in this paper will be of value in the design of bonded joints.

References

[1] Ahluwalia, K. S., "Stress Analysis of Double Shear Bonded Joints by the Finite Element Method," Master's thesis, Louisiana State University, Engineering Science Dept., Baton Rouge, La., Jan. 1969.

[2] Bikerman, J. J., *The Science of Adhesive Joints*, Academic Press, New York, 1968.

[3] Cornell, R. W., "Determination of Stresses in Cemented Lap Joints," *Journal of Applied Mechanics*, Vol. 75, Sept. 1953, pp. 355–364.

[4] Feher, S., "Research Study of Common Bulkhead and Manufacturing Technology Improvement Program for Saturn States," Contract NAS8-20376, June 23, 1967, Whittaker Corp., San Diego, Calif.

[5] Goland, M. and E. Reissner, "The Stresses in Cemented Joints," *Journal of Applied Mechanics*, Vol. 66, 1944, pp. A-17–27.

[6] Nadler, M. A. and S. Y. Yoshino, "Adhesive Joint Strength as Function of Geometry and Material Parameters," Society of Automotive Engineers, Aeronautic and Space Engineering and Manufacturing Meeting, Paper 670856, Los Angeles, Calif., Oct. 2–6, 1967.

[7] Perry, H. A., "How to Calculate Stresses in Adhesive Joints," *Product Engineering*, McGraw-Hill, New York, July 1958, pp. 64–67.

[8] Sherrer, R. W., "Stresses in a Lap Joint with Elastic Adhesives," U.S. Dept. of Agriculture, Forest Service 1864, Sept. 1957.

[9] Tombach, H., "Adhesive Joints," *Machine Design*, Vol. 29, No. 7, April 1957, pp. 113–120.

[10] Wegman, R. F., et al., "Adherend Mechanical Properties Limit Adhesive Bond Strengths," *Society of Aerospace Material and Process Engineers Journal*, Vol. 4, April–May 1968, pp. 68–72.

[11] Wilson, E. L., "Arbas" from short course *Matrix and Finite Element Structural Analysis*, University of California, Berkeley, 1967.

[12] Wooley, G. R., "Stress Analysis of Bonded, Single, Lap Joints by the Finite Element Method," Master's thesis, May 1970, Engineering Science Dept., Louisiana State University, Baton Rouge, La.

[13] Zienkiewicz, O. C. and Y. K. Cheung, *The Finite Element Method in Structural and Continuum Mechanics*, Chap. 3, McGraw-Hill, London, 1967.

OCTOBER 1971 J. AIRCRAFT VOL. 8, NO. 10

Dynamic Performance Characteristics of Mixed and Unmixed Turbofan Engines

FRANZ N. FETT*
The University of Tennessee Space Institute, Tullahoma, Tenn.

Mixed and unmixed type turbofans, having identical rotating components and thermodynamic cycles, are compared in terms of transient characteristics and steady-state off-design operation. Effects of step changes in fuel flow rate, nozzle area, inlet pressure, ambient temperature and air bleed are illustrated on both the fan and compressor operating maps. Results show significant differences in the dynamic behavior of the mixed and unmixed turbofan engines without the influence of an engine control. Off-design steady-state operating points are also different. Both effects are more pronounced in the low-pressure fan than in the high-pressure compressor. Such characteristics are important in the design of a compatible engine control unit.

Introduction

THE turbofan engine in its mixed and unmixed form is the most common engine in modern civil aircraft. Mixed augmented turbofans are finding many applications as the power plant for supersonic military aircraft. Thermodynamic design and turbofan cycle optimization have been studied extensively. Pearson[1] and others have explained the advantages of the mixed turbofan engine. References 2 and 3 summarize the methods of thrust augmentation by energy transfer and mixing between the primary and the secondary air flows. In general, the turbofan cycle is superior to the basic turbojet engine. However, the performance advantages of the mixed to unmixed turbofan is only a few percent.

Engine dynamic characteristics, important in design of compatible control units, are quite different for turbojets and turbofans. Also, significant differences between the flow dynamics of mixed and unmixed turbofan can be recognized. In this paper the steady-state off-design and transient behavior of these two types of turbofan engines are discussed. Both models used are two-spool fixed geometry engines with identical rotating components and identical thermodynamic cycle parameters. The analytical method of Refs. 4 and 7 is applied to investigate the transient behavior with step changes in fuel flow rate, nozzle area and other disturbances which are characteristic in modern engine applications. Reference 5 shows a similar engine comparison for acceleration and deceleration under command input and in closed loop.

Received April 6, 1970, revision received September 18, 1970.

* Visiting Assistant Professor, now Fried. Krupp Gmbh, Essen, Germany.

Engine and Control Inputs

The construction of both turbofans investigated are compared in Fig. 1, with the upper half illustrating the mixed

Table 1 Common data, sea level static conditions

Compression ratio	$\pi_{CI} = 18.5$
Fan pressure ratio	$\pi_{CII} = 2.4$
Turbine inlet gas temperature	$T_{t3} = 1400°K$
Primary mass flow	$\dot{m} = 31.2$ kg/sec
Bypass ratio	$\lambda = 0.59$
Inertia, low-pressure rotor	$I_{LP} = 2.48$ kg m^2
Inertia, high-pressure rotor	$I_{HP} = 1.95$ kg m^2
Thrust	$F = 2700$ daN

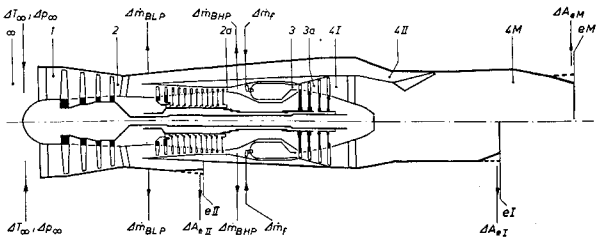

Fig. 1 Mixed and unmixed turbofan models.

engine and the lower half the unmixed engine. All components are identical except for the ducting and exit nozzles. Thermodynamic cycle data and the mass flow rates of the primary and the secondary streams are also equal (see Table 1). The unmixed engine has no mixing chamber, therefore the expansion of the fluid occurs in two separate nozzles. The thurst of the mixed engine is insignificantly higher than the unmixed case.

Input parameters that are considered to affect both power plants are marked on Fig. 1 and defined in Table 2. Engine reactions, resulting from the influence of the parameters, can be superimposed as long as the input magnitudes are kept small and only one input is changed at a time. This system corresponds to the case of an engine without a control unit which is operated with fixed input variables. Knowledge of the engine transient behavior is necessary for the design of the control unit which must modify the system dynamics to meet the requirements.

Calculation Procedure

The analysis is based on a detailed description of the thermodynamic and flow relationships inside the engine (see Appendix). According to Refs. 4 and 7, the information system needed can be gained by formulating the continuity equation and the energy equation for all the stations where a change of mass flow rate or of the enthalpy level takes place. These links can be easily formulated by the aid of mass flow and energy flow diagrams, which provide a clear picture of these rather complex relations. Figure 2 shows the common energy flow diagrams for both bypass engines. These equations of continuity and energy flow include the formulation of the steady-state conditions as well as of the dynamic terms.

The dynamic terms are the mass capacity of the volumes and the energy capacities of the gas volumes (potential and thermal energy), of the rotors (kinetic energy in the rotors, of which terms alone are indicated in Fig. 2) and of the material of the hot components for the engine (thermal energy). Particularly for small inputs and for transients in the order of magnitude of a few seconds, the short-time and long-time influence of accumulation effects in the volumes and material can be neglected. Also, the ignition delay of the combustion and the propagation velocity of informations through the engine are not considered in this simplified calculation.

Further necessary information is the individual relations between the enthalpy differences of the components and their inlet temperature, pressure ratio and efficiency. The equality of the products of the pressure ratios of the compressing and expanding parts of the engine, formulated for the primary and secondary flow, completes the description of the cycle. Furthermore, the corrected variables of the components are to be related to the equivalent absolute variables.

Table 2 Input parameters

ΔT_∞	ambient temperature change
Δp_∞	ambient pressure change
$\Delta \dot{m}_{BLP}$	low-pressure compressor (fan) airbleed
$\Delta \dot{m}_{BHP}$	high-pressure compressor airbleed
$\Delta \dot{m}_f$	fuel flow rate change
ΔA_{eM}	nozzle exit area change, mixed engine
ΔA_{eI}	nozzle exit area change, primary flow of unmixed engine
ΔA_{eII}	nozzle exit area change, secondary flow of unmixed engine

With the aid of the characteristic maps of the components, the mass flow rates of inlet, compressors, turbines and nozzles are formulated as a function of their individual inlet values. From this the flow characteristic is obtainable in the neighborhood of the operating point to be investigated. The local trend of the component efficiencies can be included in a similar manner.

If furthermore the thrust, the specific fuel consumption, and other desired characteristic performance values are added, an extensive system of equations is available which represents a complete description of the off-design behavior of an engine, including the transient effects.

The solution of the system can be achieved by iterative stepwise calculation, or for small inputs like disturbances it can be solved directly after linearization. The results can be superimposed for different inputs. In the case used here, the solution of the system of differential equations can be performed by matrix inversion and matrix multiplication.

The transfer functions of all variables are now available as a function of the inputs, which are introduced in Fig. 1. They are of second order and have the form

$$x_i(s) = \left\{ \sum_{k=1}^{m} [c_{i,k} + c_{i,k}{}^{*}s + c_{i,k}{}^{**2}s^2] \Big/ (1 + T_1 s + T_2{}^2 s^2) \right\} y_k(s) \quad (1)$$

where x_i is any dependent and y_k any independent variable, $c_{i,k}$ the transfer factor, $c_{i,k}{}^{*}$ and $c_{i,k}{}^{**}$ the time constants of the numerator and T_1 and T_2 the time constants of the denominator; m is the number of independent variables and s the complex variable of the Laplace transform. Knowing this, the transient functions of all engine variables (all gas temperatures, pressures, mass flow rates, speeds, corrected parameters and thrust) can be calculated. These transient

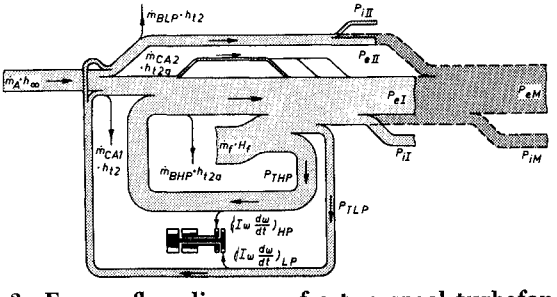

Fig. 2 Energy flow diagram of a two-spool turbofan engine with and without mixing. h_t = stagnation enthalpy, P_T = turbine power, H_f = lower heat value, P_i = kinetic engine power, $\dot{m}_A$ = air mass flow rate, P_e = thermal power of exit stream, $\dot{m}_{CA}$ = cooling air mass flow, ω = angular velocity.

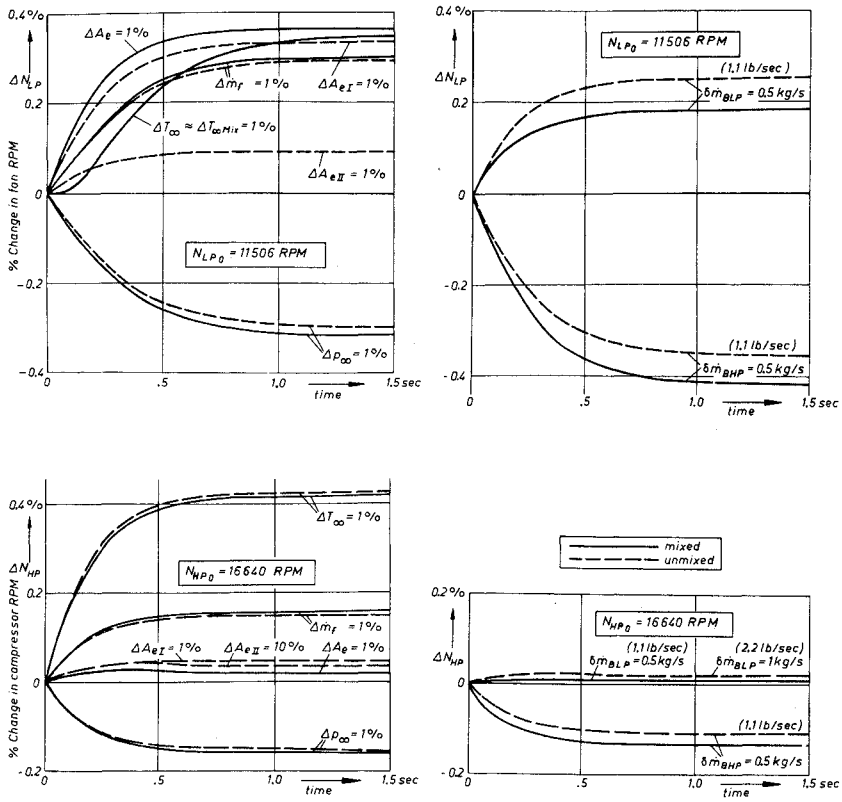

a) Low-pressure spool.

b) High-pressure spool.

Fig. 3 Transient rotor speeds.

functions describe the steady-state off-design as well as the transient operation.

Transient Functions

The time behavior of the two engine systems can primarily be evaluated by means of the time constants T_1 and T_2 and the damping factor. Table 3 shows these values for the mixed and unmixed turbofan engine. The numerical values are scarcely different. This is no surprise since all the parameters that affect the time behavior are identical for both engine types: the inertias of the rotors as well as the thermodynamic data and mass flow rates through the rotors, which determine the acceleration torques. The step input responses of the various variables that can be obtained from the transfer function, Eq. (1), gives a much clearer picture of the physical events.

Figures 3–6 give several examples. The magnitude of the actual speeds of the low-pressure and high-pressure rotors N_{LP} and N_{HP} (Fig. 3), the turbine inlet temperature T_{t3} (Fig. 4), the thrust F (Fig. 5), and the bypass ratio λ (Fig. 6) are plotted as a function of time for inputs of various manipulated and disturbance variables.

Since the rotor has an inertia, an instantaneous change of the rotor speed requires an impossibly large torque. Because the available torque is finite, the coefficients $c_{i,k}$**, which indicated the initial step of the transient, must be zero for the actual rotational speeds. That means the transient functions of the speeds are zero at time zero and have a finite slope as shown in Fig. 3. This is not the case with the corrected speeds and in general not for all other dependent variables.

The transient turbine inlet temperature (Fig. 4) and thrust (Fig. 5) functions of both engine types are nearly identical for some inputs. In other cases these transient values are different but the final values are identical. However, the differences in the actual mass flow rates and therefore in bypass ratio λ (Fig. 6) are remarkable.

Changes of the bypass ratio illustrate that the secondary cycle of a mixed bypass engine is highly affected during changes of load and under all kinds of inputs. The reason for this intensive influence is the immediate and almost instantaneous feedback through the bypass duct. All pressure deviations that travel downstream in the core engine and enter the mixing chamber are transmitted undiminished to the pressure side of the fan, which has to adapt itself. Pure temperature deviations act indirectly by changing the nozzle flow conditions. This feedback effect on the secondary cycle seems to be particularly large because of the comparatively low bypass ratio of the engines studied.

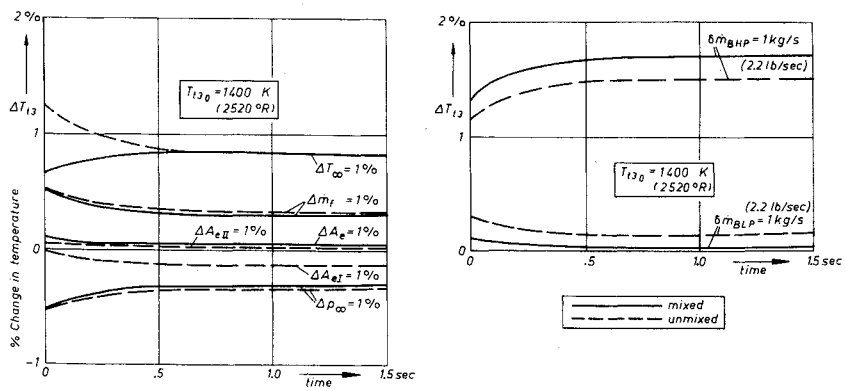

Fig. 4 Transient turbine inlet gas temperature.

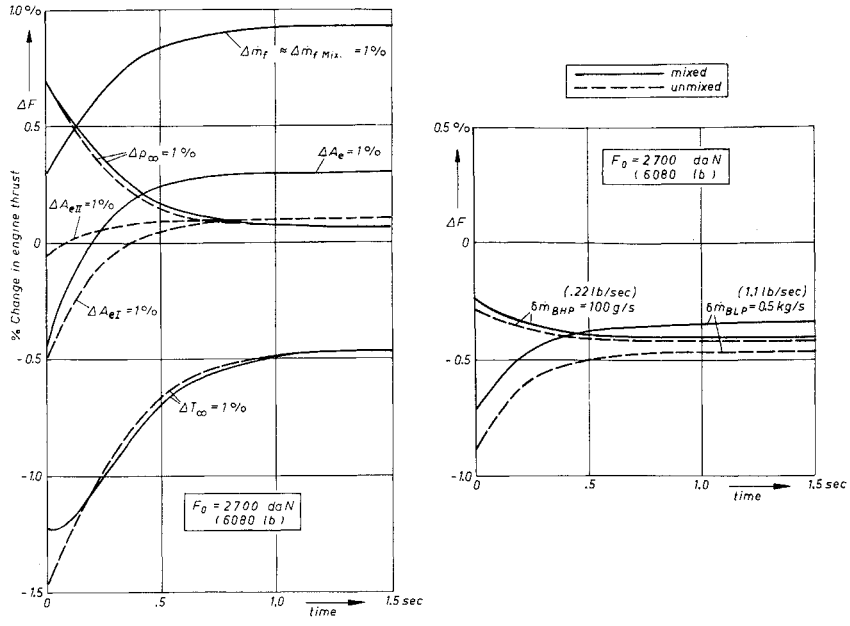

Fig. 5 Transient engine thrust.

A similar effect is seen in afterburning mixed turbofan engines where a change in the afterburner conditions acts unretarded on the fan[6] and causes considerable surge difficulties if the common nozzle is not suitably varied immediately. As discussed later, the afterburning mixed engine studied suffers a 60% decrease of its fan compressor surge margin if the afterburner fuel flow is increased by 10%.

Fan and Compressor Operation

Particularly clear is the difference in the performance of mixed and unmixed bypass engines if the deviations from the operating point are considered in the fan and compressor maps. Here the continuous change of the most important parameters such as pressure ratio π, corrected mass flow rate $\dot{m}\theta^{1/2}/\delta$, and corrected speed $N/\theta^{1/2}$, can be seen together. At the same time, the stability margin vs surge can be evaluated and the steady-state operating lines for the different inputs can be constructed. Figures 7–9 reproduce the time-dependent and steady-state path of the operating point P on the low-pressure fan and high-pressure compressor maps for various inputs. The reaction of both engines without control units are shown.

Figure 7 contains the displacement of the operating points under stepwise increases of main engine fuel flow $\Delta\dot{m}_f$ and the ambient temperature ΔT_∞. The fan again shows the largest differences. The transient functions and steady-state operating points differ widely from each other for the same inputs. The connecting lines between the origin and the new operating points produce, therefore, completely different operating lines which have different slopes and a different relationship to the surge line. The high-pressure compressor has a nearly identical operating line for both engines; however, the transients as well as the new steady-state operating points are considerably different.

Table 3 Comparison of time constants and damping factor

	Mixed	Unmixed
Time constant T_1	0.3818 sec	0.3891 sec
Time constant T_2	0.1971 sec	0.1979 sec
Damping factor D	0.9677	0.9835

A stepwise increase of the ambient pressure (which is probably the opposite of what occurs in actual practice) is illustrated in Fig. 8 for both engines. In the same set of figures the influence of an increase in nozzle area is shown for the common exit nozzle of the mixed engine and for both nozzles of the unmixed turbofan. This last comparison is not

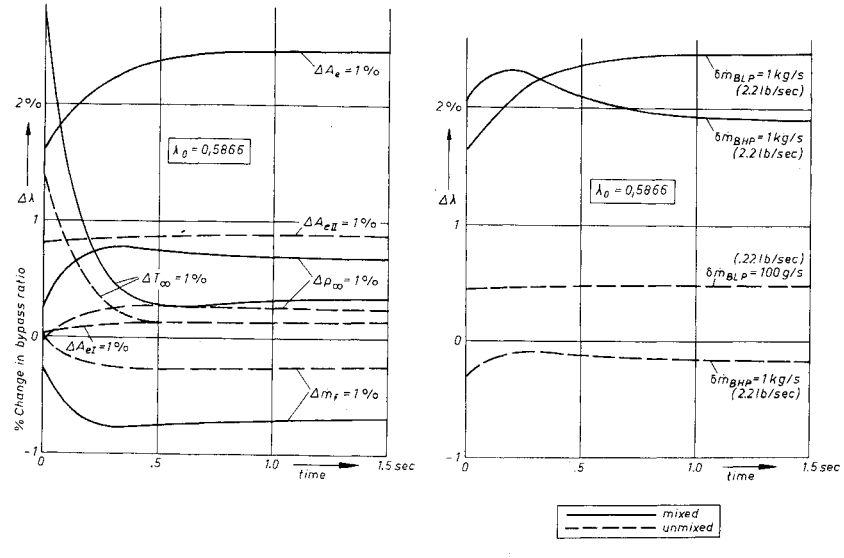

Fig. 6 Transient bypass ratio.

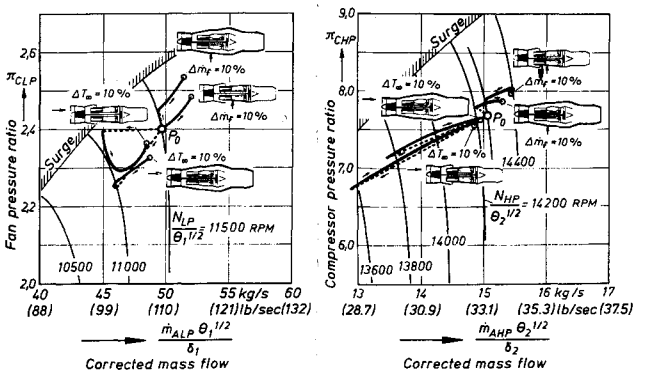

Fig. 7 Fan and compressor operation with step increases in the main engine fuel flow rate $\dot{m}_f$ and ambient temperature T_∞.

completely legitimate since the inputs are not really the same. The purpose of the use of a nozzle area change, however, is identical, and the different engine reactions have to be well understood if these inputs are to be used as manipulated variables of a control cycle. The corresponding steady-state operating lines are not at all common.

The decrease in nozzle area for the mixed turbofan also represents what happens to fan surge margin of an afterburning turbofan when afterburner fuel flow is rapidly increased. As previously mentioned, a 60% reduction in fan surge margin is indicated for the engine studied if it had an afterburner and its fuel flow were increased by 10%.

Air bleed has an important task for stabilization of VTOL aircraft during the takeoff, transition and landing phases. Air bleed behind the high-pressure compressor causes about 20 times higher thermal loading of the turbine blades than low-pressure bleed. However, the high-pressure bleed is preferred in practice, since its air ducting is considerably lighter. The paths of the operating line under air bleed are shown in Fig. 9 for both engines.

The effect of air bleed behind the fan of the unmixed engine is identical with the nozzle area change of the secondary cycle. It can further be recognized that the method of low-pressure bleed can be used as an effective mean to unburden the fan of a mixed engine during critical conditions of operation.

In interpreting the results, it has to be considered that the fan and compressor maps include only corrected variables. The changes of the actual variables of speed, mass flow rate and pressures may deviate very much from the corrected ones. This statement holds always for the high-pressure compressor and is even true for the fan if the ambient data are changed.

Summary

The characteristic transient behavior of identical turbofan engines operating in the mixed and unmixed modes has been discussed. Reactions of the engines to some stepwise disturbance inputs which are characteristic for modern engine application are compared without influence of a control unit. The results obtained show minor impact on the behavior of the engine core of both types. The reaction of the low-pressure part, however, must be considered in greater detail since the same variables can have very different transients, and also, the operating lines of both engines are rather different.

Appendix: Some Details of Calculation Procedure

The system of equations can be shown in an abbreviated form as follows and may generally be applied to any type of propulsion unit.

1) The laws of mass, Eq. (2), and energy conservation, Eq. (3), must be formulated as often as mass flows and energy flows associate or dissociate. V_{ch} is the volume

$$\Sigma\dot{m} + [V_{ch}d\rho_{ch}/dt] = 0 \tag{2}$$

$$\Sigma\dot{m}h + [d(m_{ch}h_{ch})/dt] + [I\omega d\omega/dt] + [m_e dh_e/dt] = 0 \tag{3}$$

of the combustion chamber, ρ_{ch} the density, m_{ch} the mass and h_{ch} the enthalpy of the gas in the chamber, m_e is the mass of the heated engine parts like turbine blades, discs, and casing, and h_e the enthalpy of these parts. The number of equations of this type is a function of the type of propulsion unit. The terms placed within brackets in Eq. (2) take into account the time-dependent mass capacity of the volumes of the combustion chamber. The bracketed terms in Eq. (3) take into account the time-dependent energy capacity of the rotors, the gas volumes and hot structures.

2) Equation (4) links the enthalpy differences of the components with their pressure ratio π and efficiency η, as well as the inlet temperature T of the fluid. The number of equations is subject to the number of components.

$$\Delta h = \Delta h(\pi,T,\eta) \tag{4}$$

3) Equation (5) equates the products of the pressure conditions of compression and expansion for the basic engine and for the bypass

$$\Pi\pi_{\text{compr.}} - \Pi\pi_{\text{expans.}} = 0 \tag{5}$$

4) Equation (6) describes the flow characteristics of the engine components with a deviation from the condition of steady state

$$\dot{m}_{\text{corr}} = \dot{m}_{\text{corr}}(\pi,N,\alpha) \tag{6}$$

$\dot{m}_{\text{corr}}$ being the corrected mass flow rate and α the blade angle.

5) Equation (7) links the corrected values with the corresponding dimensional ones

$$\dot{m}_{\text{corr}} = \dot{m}_{\text{corr}}(\dot{m},\pi,T) \tag{7}$$

6) Equation (8) illustrates by analogy to Eq. (6) the efficiency trend of the components with a deviation from the steady state

$$\eta = \eta(\dot{m}_{\text{corr}},\pi,N_{\text{corr}}) \tag{8}$$

7) The terms in Eq. (9) denote that the trend of various performance data will also be of particular interest

$$F,SFC,\ldots = F,SFC,\ldots\,(x_i,y_k) \tag{9}$$

With the information supplied by Eqs. (2–7), a soluble system of equations is obtained if the component efficiencies in the vicinity of the operation point to be examined are assumed to be constant. If, however, they are introduced,

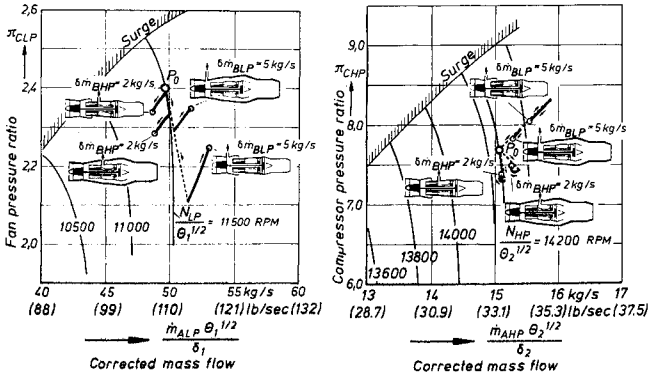

Fig. 8 Fan and compressor operation with step changes in exit nozzle areas A_e and ambient pressure p_∞.

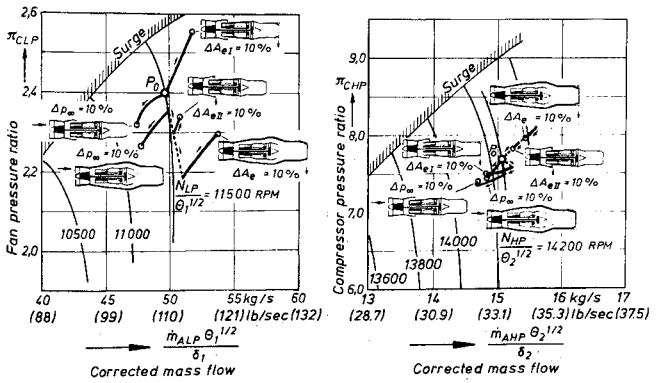

Fig. 9 Fan and compressor operation with step increases in low-pressure air bleed $\dot{m}_{BLP}$ and high pressure air bleed $\dot{m}_{BHP}$.

according to Eq. (8), as variables, the accuracy of calculation is improved. Eq. (9) enables the determination of any variable of additional interest, which may be formulated from the variables already introduced in the system from Eqs. (2–8).

Of particular importance are the instationary elements of the system of equations, which influence the transient characteristics of the dependent variables, but not their final steady-state value. The effect of these shares is dependent upon the storage capacity of the components and structures concerned and on the time required to fill and drain the capacity.

For the determination of all nonstationary processes caused by brief interferences in the order of a few seconds, it is sufficient to take into account merely the energy accumulating rotor to obtain a satisfactory approximation.

References

[1] Pearson, H., "Mixing of Exhaust and Bypass Flow in a Bypass Engine," *Journal of the Royal Aeronautical Society*, Vol. 66, Aug. 1962, pp. 528–530.

[2] Heiser, W. H., "Thrust Augmentation," *Transactions ASME, Ser. A*, Vol. 89, 1967, pp. 75–82.

[3] Dettmering, W. and Fett, F., "Methoden der Schuberhöhung und ihre Bewertung," *Zeitschrift für Flugwissenschaften*, Vol. 17, No. 8, Aug. 1969, pp. 257–267.

[4] Fett, F., "The Dynamic Behavior of Jet Engines under External and Internal Action," *Advanced Components for Turbojet Engines, Part 2*," Paper 31, AGARD Conference Proceedings 34, Sept. 1968.

[5] Bauerfeind, K., "Die Berechnung des Übertragungsverhaltens von Turbo-Strahltriebwerken unter Berücksichtigung des instationären Verhaltens der Komponenten," *Luftfahrttechnik-Raumfahrttechnik*, Vol. 14, No. 5 and No. 6, May and June 1968, pp. 117–124 and pp. 143–151.

[6] Greathouse, W. K., "Blending Propulsion with Airframe," *Space/Aeronautics*, Vol. 50, No. 6, Nov. 1968, pp. 59–68.

[7] Fett, F., "Das Regelverhalten von Strahltriebwerken," *Forschungsberichte des Landes Nordrhein-Westfalen*, No. 2065, Westdeutscher Verlag, Köln und Opladen, 1970.

OCTOBER 1971 J. AIRCRAFT VOL. 8, NO. 10

Exhaust Nozzle Drag: Engine vs Airplane Force Model

DAVE BERGMAN*
Convair Aerospace Division, General Dynamics Corporation, Fort Worth, Texas

A nozzle model which utilizes interchangeable internal and external parts was tested at high subsonic Mach numbers. Differences in nozzle drag brought about by the use of force- or reference-model exhaust conditions in contrast to engine conditions were investigated. In addition to typical designs, a number of alternative force-model nozzle (the type used in flow-through nacelles) variations were tested and evaluated. In general, force-model nozzle drag was found to be far different from that of the engine nozzles; however, some force-model variations did simulate the effects of engine flow at discrete operating conditions.

Nomenclature

A = cross-sectional area
C_D = boattail pressure drag coefficient (Drag/q_0A_m)
C_P = boattail pressure coefficient, $(P - P_0)/q_0$
D,d = diameter
h = boundary-layer height
L = length of boattail
M_0 = freestream Mach number
NPR = nozzle pressure ratio (P_{TJ}/P_0)
P,P_0 = local and freestream static pressure
P_{TJ} = exhaust jet total pressure
q = dynamic pressure
R = radius

Subscripts

B,b = boattail terminal plane
J = jet
M,m = maximum
0 = freestream
T = total

Introduction

AIRPLANE performance measurements, particularly those made during design and development stages, are acquired by applying a combination of experimental and analytical techniques rather than by using one specific device. This approach must be taken because, when considering an entire airplane configuration, each of these techniques has severe limitations, and the sole use of either will compromise accuracy in predicting airplane performance. As a result, an approach which systematically integrates both analytical and test results is normally used.

Presented as Paper 70-668 at the AIAA 6th Propulsion Joint Specialist Conference, San Diego, Calif., June 15–19, 1970; submitted June 29, 1970; revision received September 30, 1970.

* Propulsion Engineer, Aerospace Technology Department.